A novel animal model to investigate fractionated radiotherapy-induced alimentary mucositis: the role of apoptosis, p53, nuclear factor-κB, COX-1, and COX-2

Ann S.J. Yeoh,[1,3] Rachel J. Gibson,[1,3] Eric E.K. Yeoh,[2,3] Joanne M. Bowen,[1,3] Andrea M. Stringer,[1,3] Kar A. Giam,[2] and Dorothy M.K. Keefe[1,3]

Departments of [1]Medical Oncology and [2]Radiation Oncology, Royal Adelaide Hospital; [3]Discipline of Medicine, University of Adelaide, Adelaide, South Australia, Australia

Abstract

Radiation-induced mucositis is a common and serious side effect of radiotherapy. Molecular mechanisms of mucosal injury, however, are still poorly understood and extremely difficult to study in humans. A novel Dark Agouti rat model using fractionated radiotherapy to induce mucositis has been developed to investigate the occurrence of alimentary mucosal injury. Twenty-four Dark Agouti rats were randomly assigned to receive either fractionated radiotherapy or no radiotherapy. The irradiated rats received a fractionated course of abdominal radiotherapy at 45 Gy/18 fractions/6 weeks treating thrice weekly (i.e., at a radiation dose of 2.5 Gy per fraction). After each week of radiation, a group of irradiated rats was killed. Histomorphology and mucin distribution in the alimentary tract was investigated. The terminal deoxynucleotidyl transferase–mediated dUTP nick end labeling assay was used to examine apoptosis in the colon and jejunum, and intestinal morphometry was used to assess villus length, crypt length, and mitotic crypt count. Immunohistochemistry of p53, nuclear factor-κB, cyclooxygenase (COX)-1, and COX-2 was also done. The fractionated radiotherapy course induced alimentary mucositis from week 1, with more severe injury seen in the small intestine. The hallmark appearance of apoptosis was present in the crypts of the small and large intestine. In the jejunum and colon, goblet cell disorganization and degeneration was obvious and crypt mitotic counts were severely depleted throughout the treatment. Expression of p53, nuclear factor-κB, COX-1, and COX-2 was increased in the irradiated intestinal sections. Fractionated radiation-induced alimentary mucositis has been effectively documented in the Dark Agouti rat for the first time. Further studies investigating the molecular mechanisms underlying radiation-induced mucositis are planned to ultimately achieve anti–mucotoxic-targeted therapies. [Mol Cancer Ther 2007;6(8):2319–27]

Introduction

Mucositis, a significant dose-limiting side effect of chemotherapy and radiotherapy, may affect any region of the alimentary tract, depending on the treatment type, and lead to a broad range of symptoms, such as oral pain, stomach bloating, and severe diarrhea. The pathogenesis of mucosal injury has been the subject of intense research, as elucidating the mechanisms that underlie mucosal injury would lead to treatments targeted to preventing the loss of mucosal barrier functions that lead to these debilitating and painful side effects of antineoplastic therapy.

Studies investigating chemotherapy-induced mucositis have been instrumental in identifying the early changes to the mucosa (1–5). Using a well-established rat model, mucositis has been induced by the administration of a chemotherapeutic agents, including methotrexate (2, 4), irinotecan (CPT-11; refs. 1, 3, 6), and 5-fluorouracil (7). These studies have shown that mucositis in this model mimics the symptoms and mucosal damage that occur in mucositis occurring in humans (1–5). In these studies, the earliest effect of chemotherapy was a 7-fold increase in apoptosis in intestinal crypts within 24 h of treatment. Apoptosis in the crypts of the small intestine preceded hypoplastic villus atrophy, with intestinal hypoplasia peaking between 2 and 4 days after treatment (5). This finding led to the investigation of molecular mechanisms that underlie the apoptosis and crypt hypoproliferation (8–10) and gene changes that occur during mucositis (6). Consequently, palifermin (keratinocyte growth factor), which enhances the regenerative capacity of epithelial tissues, has been evaluated and is now the first agent approved for use in prevention of oral mucositis for patients treated with high-dose chemotherapy with or without radiation therapy (11).

A five-phase pathobiological model of oral mucositis proposed by Sonis (12–14) explains the current hypothesis of the mucosal barrier injury thought to occur when

Received 2/19/07; revised 5/17/07; accepted 6/29/07.

Grant support: Conservation Council of South Australia fellowship (R.J. Gibson).

The costs of publication of this article were defrayed in part by the payment of page charges. This article must therefore be hereby marked *advertisement* in accordance with 18 U.S.C. Section 1734 solely to indicate this fact.

Requests for reprints: Ann S.J. Yeoh, Mucositis Research Group, Dame Roma Mitchell Cancer Research Laboratory, Level 4, Hanson Institute, Frome Road, Adelaide, South Australia 5000, Australia.
Phone: 61-8-8222-3547; Fax: 61-8-8222-3217.
E-mail: ann.yeoh@imvs.sa.gov.au

doi:10.1158/1535-7163.MCT-07-0113

chemotherapy or radiotherapy is administered (11, 13, 14). However, there are differences in severity and onset of symptoms between both types of antineoplastic therapy. This can be attributed to systemic chemotherapy regimens that consolidate the insult into a short, but intense, time frame, whereas the fractionated dosing regimen of radiation therapy in small daily doses causes milder but cumulative damage to the mucosa, which may be sustained. This five-phase model has also been used to postulate the basis of mucosal injury occurring in the rest of the alimentary tract. It is hypothesized that mechanisms of mucosal injury along the whole length of the alimentary tract from mouth to anus would be the same or similar (15, 16). Differences in manifestation of symptoms are attributed to the differences between functional, immunologic, and microbiological differences between the different regions of the alimentary tract (11, 13, 14). The patterns of mucositis and healing also vary according to the antineoplastic treatment given.

Further understanding of mucositis requires the detailed investigation of other causes of mucosal barrier injury and the protective mechanisms that limit nontumor cell death. Radiation-induced mucositis is the less researched area in this field. Nonetheless, the proportion of patients reporting oral and gastrointestinal mucositis symptoms are significant, with 30% to 60% of head and neck cancer patients receiving radiation therapy reporting symptoms (17) and 75% of patients reporting gastrointestinal mucositis symptoms when receiving pelvic irradiation (18, 19). When chemotherapy and radiation therapy are combined, at least 95% of patients report some form of mucositis (20). Radiation therapy, particularly the conventional multifraction radiation therapy regimens used widely for treatment of oncological patients today, is therefore an important cause of mucosal barrier injury.

Animal models for research in mucosal barrier injury form the platform in which basic understanding of the molecular mechanisms of mucosal barrier injury is sought. There has yet to be an animal model developed to investigate the effect of the short-term and long-term fractionated radiation therapy regimen on the mucosal barrier of the alimentary tract.

In this novel study showing mucositis in the Dark Agouti rat, 24 female rats underwent a schedule of fractionated radiotherapy localized to the abdomen. Both short-term and long-term fractionated regimens were used to closely mimic the clinical situation as experienced by patients. In this rat irradiation pilot study, histologic variables and the role and changes of molecular key players in response to ionizing radiation were examined to determine the occurrence of alimentary mucositis.

Materials and Methods

Ethics

All procedures in this pilot animal study were reviewed and approved by the Animal Ethics Committees at the Institute of Medical and Veterinary Sciences, Adelaide and at the University of Adelaide. The work and animal care complies with the National Health and Medical Research Council Code of Practice of Care for Animals in Research and Training (2004). As the Dark Agouti rat had not been previously used in radiation trials, the cohort size was kept to a minimum to minimize unnecessary animal deaths from severe side effects should they have occurred.

Animals

Twenty-four female Dark Agouti rats (University of Adelaide Breeding Facility), weighing 150 to 170 g, were used. The animals were housed under environmentally controlled conditions with a 12-h dark and 12-h light cycles. The rats were housed in groups of five with free access to water and standard rat chow.

Irradiation Protocol and Experimental Design

Twenty-four Dark Agouti rats were randomly assigned into six groups of three to receive fractionated radiation, and the remaining six rats formed the control group that remained untreated. The rats in the irradiated groups received a fractionated course of radiotherapy at a radiation dose of 2.5 Gy/fraction with a total of 45 Gy/18 fractions/6 weeks treating thrice weekly as an incident dose. Radiation was administered using a Phillips Deep X-ray unit (RT 250, Phillips) with a half value layer of 2-mm copper and focus-skin distance of 50 cm. Dosimetry and irradiation geometry were calibrated before radiation. Immediately before each dose of radiation, the rats were placed in a purpose-built container and anesthetized using 3% halothane in 100% oxygen. The control rats were also anesthetized and placed in the purpose-built container but did not receive radiation. Radiation was limited to the abdomen of the rat by appropriate lead shielding of the head, thorax, lower pelvis, and all extremities. Animals were monitored carefully twice daily throughout the experimentation period, increasing to four times daily if needed, with daily weighing, inspection of feces, and assessment of behavioral characteristics. Clinical record sheets were filled out accordingly. After each week of radiation, a group of irradiated rats was sedated and then exsanguinated via a cardiac puncture and killed via cervical dislocation. The alimentary tract was removed, and the small and large intestine was flushed using cold isotonic saline. Specific samples in the alimentary tract were removed (jejunal region taken at 30% of small intestinal length when measured from pylorus, and colonic sections were taken at midlength of the dissected large intestine). Tissue specimens were fixed in Clarke's fixative [75% (v/v) ethanol/25% (v/v) glacial acetic acid] for morphometry and 10% neutral formalin for processing and fixing in paraffin for histologic and immunohistochemical analysis.

Histologic and Goblet Cell Examination

Standard H&E and Alcian blue and periodic acid-Schiff staining methods have been previously established and described (21).

Intestinal Morphometry

Methods for analyzing intestinal morphometry have been described previously (2). In brief, small sections (1 cm)

of jejunum stored in 70% ethanol after fixing in Clarke's fixative for 24 h were rehydrated and hydrolyzed in 1 mol/L HCl for 7 min at 60°C. After two washes in double-distilled water, the tissues were stained with Schiff's reagent for 45 min before being microdissected. Tissues were mounted in 45% acetic acid using a calibrated microscope graticule, and measurements of villus length, apical and basal widths of 15 villi, and the lengths of 15 crypts were taken. The microdissected crypts were then squashed, enabling clear identification of mitotic figures. Mitotic counts per crypt were recorded. Small pieces of colon were processed the same way, and colonic crypt length and mitotic count per crypt were recorded. All tissue assessment was conducted in a blinded fashion.

Terminal Deoxynucleotidyl Transferase–Mediated dUTP Nick End Labeling Assay

Sections (4 μm) of jejunum and colon were labeled for apoptosis using the terminal deoxynucleotidyl transferase–mediated dUTP nick end labeling (TUNEL) assay. The assay was done using the *In situ* Cell Death Detection kit (Roche). After dewaxing and rehydration, slides were immersed in a 0.1% Triton X-100 in 0.1% sodium citrate buffer for 8 min at room temperature. Following two rinses in PBS, slides were placed in a TUNEL buffer solution (150 mmol/L Tris, 0.7 mmol/L NaCaCo, 10 mmol/L $CoCl_2$, 10% bovine serum albumin, and sterile H_20) for further 10 min at room temperature. The reaction mixture was immediately placed on the sections on the slide and then left to incubate in a humidified chamber for 3 h at 37°C. Following three rinses in PBS, slides were then incubated with Converter-AP in a humidified chamber for 60 min at 37°C, after which they were rinsed in a further two changes of PBS. Fast Red chromogen (Roche) was applied for 15 min. Slides were rinsed and counterstained with hematoxylin. Apoptosis in the jejunum and colon could then be counted and expressed as apoptotic bodes per crypt. On average, 150 crypts were assessed for apoptosis in each animal.

Immunohistochemistry for Detection of p53, Nuclear Factor-κB, Cyclooxygenase-1, and Cyclooxygenase-2

Immunostaining was detected as described in previous studies (21). p53 (Novacastra) is a mouse monoclonal antibody, NF-κB p65 (F-6; Santa Cruz Biotechnology) is an affinity-purified mouse monoclonal IgG1 antibody, and cyclooxygenase (COX)-1 (M-20; Santa Cruz Biotechnology) and COX-2 (M-19; Santa Cruz Biotechnology) are purified goat polyclonal antibodies. Working dilutions for p53, nuclear factor-κB (NF-κB), COX-1, and COX-2 were 1:50, 1:2,300, 1:1,700, and 1:2,000, respectively.

In brief, serial 4-μm sections of jejunum and colon were cut and mounted on silane-coated microscope slides. Each slide was deparaffinized in xylene and rehydrated in ethanol followed by antigen retrieval in citrate buffer (pH 6.0). This was followed by endogenous peroxidase blocking in 3% H_2O_2 in methanol for 1 min. Rehydration followed, and a nonspecific protein blocking step using goat serum (20%) for p53 and horse serum (20%) for NF-κB, COX-1, and COX-2 was done. Endogenous avidin-biotin activity was blocked using the Avidin/Biotin Blocking kit (Vector Laboratories). The respective primary antibody was applied [p53 with 2% goat serum and NF-κB, COX-1, and COX-2 with 5% horse serum (Sigma)] in PBS and slides were left overnight (16 h) at 4°C in a humidified chamber. Following incubation with the primary antibody, a secondary antibody [biotinylated antimouse IgG affinity-purified antibody (Vector Laboratories)] at a dilution of 1:200 with 5% horse serum was applied for slides treated with NF-κB and p53 antibody and biotinylated antigoat IgG affinity-purified antibody (Vector Laboratories) of 1:200 dilution with 5% horse serum for slides with COX-1 and COX-2 antibody for 20 min at room temperature. Subsequently, labeling reagent ultrastreptavidin peroxidase (Signet Pathology Systems, Inc.) was applied for 20 min at room temperature. Antibody binding was visualized with 3,3′-diaminobenzidine tetrachloride (Zymed Laboratories, Inc.). This was followed by counterstaining with Lillie-Mayer's hematoxylin and the subsequent dehydration and mounting.

Analysis

All tissue analysis was conducted in a blinded fashion by one investigator (A.S.J.Y.). Histologic and goblet cell assessment was done using light microscopy. Qualitative immunohistochemical analysis was done also using light microscopy to capture digital photographs of the stained

Table 1. Body weight, weight of small intestine, and weight of large intestine in female Dark Agouti rat treated with fractionated radiation at respective kill day

Treatment group	Body weight (g)	Small intestine (g)	Large intestine (g)
Week 1	152.4 ± 4.3*	4.4 ± 0.3	1.2 ± 0.0
Week 2	158.9 ± 8.5*	5.1 ± 0.3	1.37 ± 0.3
Week 3	171.6 ± 3.1*	4.7 ± 0.2	1.37 ± 0.2
Week 4	168.8 ± 2.8*	5.3 ± 0.0	1.55 ± 0.2
Week 5	175.5 ± 12.8*	5.1 ± 0.3	1.45 ± 0.1
Week 6	170.9 ± 6.2*	4.7 ± 0.2	1.50 ± 0.4
Untreated controls	195.1 ± 5.6*	4.9 ± 0.7	1.42 ± 0.1

NOTE: Data are given as mean ± SD (g). Weights of irradiated rats were significantly less compared with the weights of the untreated controls. There was no significant difference in small and large intestine weights.
*Weeks 1 to 3, $P < 0.001$; week 4, $P < 0.0018$; week 5, $P < 0.027$; week 6, $P < 0.0013$.

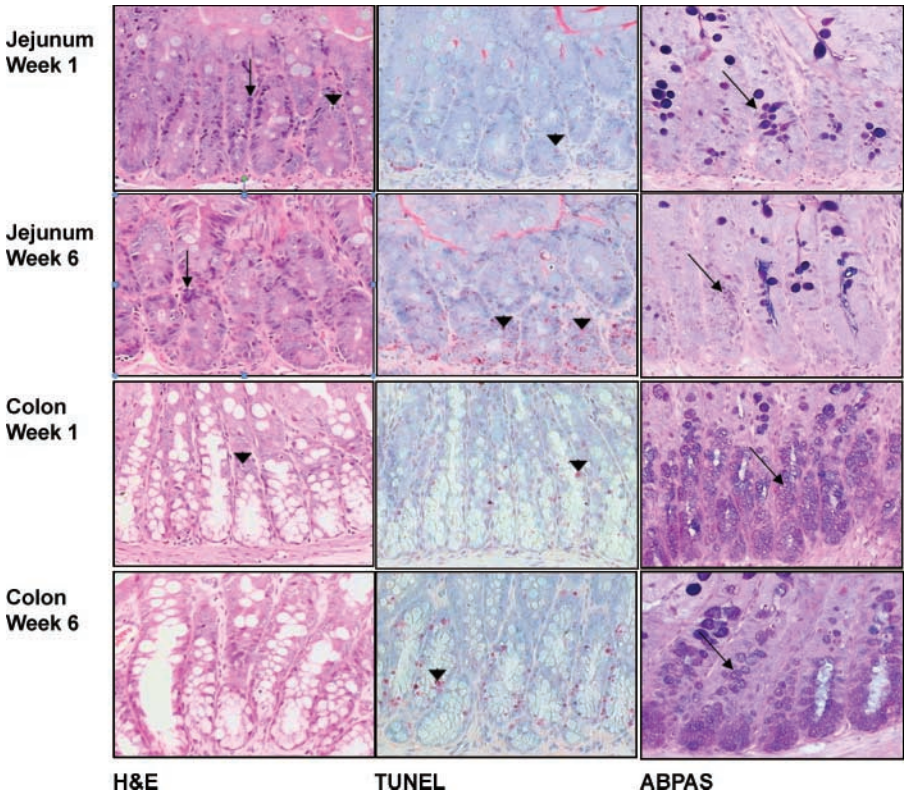

Figure 1. Histopathologic changes and apoptosis as documented by H&E, TUNEL assay, and goblet cell stain [Alcian blue and periodic acid-Schiff (*ABPAS*)] during the 6-wk course of radiotherapy. *Straight arrows in H&E-stained sections,* prominent pyknotic nuclei. *Arrowheads in the H&E and TUNEL sections,* apoptotic cells. Apoptosis was a prominent finding in this animal study, and the TUNEL assay was used to quantify these apoptotic cells. *Slanted arrows in the ABPAS-stained sections,* disintegration of goblet cells (in week 1 of jejunum and colon sections) and, later on at week 6, a loss of goblet cells.

tissue. p53, NF-κB, and COX-2 expression was scored based on the intensity of the staining as follows: 0, no staining; 1, weak staining; 2, moderate staining; 3, moderate-intense staining; and 4, intense staining. This qualitative assessment of staining has previously been validated by published grading systems and is routinely used in our laboratory (22–24). There was a consistent level of staining across all the tissue sections, which allowed for any region of the tissue to be examined and recorded as an accurate representation of expression.

All statistical data were expressed as mean ± SD. The ANOVA statistical test was used to distinguish significance between data groups. Results to the ANOVA were considered statistically significant when $P < 0.05$. In all statistical tests conducted, data from weekly treatment groups were compared against data from the untreated control groups.

Results

Response to Treatment

Throughout the 6-week fractionated radiation therapy (at a radiation dose of 2.5 Gy/fraction), no animal recorded diarrhea. Irradiated rats had a slower weight gain rate compared with nonirradiated rats, with statistically significant decreases in weight when all weekly treatment

Table 2. Villus height and crypt length and mitotic count per crypt as radiation treatment progressed

Treatment group	Villus height (μm)	Crypt length (μm)	Mitoses (per crypt)
Week 1	50.8 ± 8.9	60.8 ± 8.3*	1.4 ± 1.0*
Week 2	56.8 ± 5.7	55.5 ± 7.4*	1.2 ± 0.9*
Week 3	48.6 ± 9.4†	71.0 ± 9.2*	0.6 ± 0.7*
Week 4	43.7 ± 11.3†	63.6 ± 8.8*	0.5 ± 0.7*
Week 5	55.9 ± 8.5	59.3 ± 8.7*	0.7 ± 0.6*
Week 6	51.7 ± 8.3	67.2 ± 9.7*	0.8 ± 0.8*
Untreated controls	52.5 ± 9.0†	46.6 ± 7.1*	2.7 ± 1.1*

NOTE: Data are given as mean ± SD (μm). Villus height was significantly decreased at weeks 3 and 4. Crypt length was significantly increased, whereas mitotic count was depleted throughout the duration of treatment.

* From week 1 to week 6, all P values were <0.001 when compared with untreated controls.

† Week 3, $P < 0.025$; week 4, $P < 0.001$.

Table 3. Colonic crypt length and mitotic count per crypt as radiotherapy progressed

Treatment group	Crypt length (μm)	Mitoses (per crypt)
Week 1	103.6 ± 11.5*	0.9 ± 0.9†
Week 2	146.5 ± 8.1*	0.6 ± 0.5†
Week 3	136.2 ± 18.1*	0.7 ± 0.7†
Week 4	141.8 ± 11.9*	0.4 ± 0.6†
Week 5	148.8 ± 15.4*	0.9 ± 0.7†
Week 6	119.9 ± 14.5	0.5 ± 0.6†
Untreated controls	116.1 ± 15.4*	1.7 ± 0.9†

NOTE: Data are given as mean ± SD (μm). Crypt length was significantly increased when compared with the untreated controls, and mitotic count severely decreased throughout the 6-week radiation therapy.

*From week 1 to week 5, all P values were <0.001 when compared with controls.

†From week 1 to week 6, all P values were <0.001 when compared with controls.

groups were compared with the untreated control group (weeks 1–3, $P < 0.001$; week 4, $P < 0.0018$; week 5, $P < 0.027$; week 6, $P < 0.0013$; Table 1). No other obvious side effects were noted. No significant difference was noted in the weights of the small and large intestine throughout the 6-week period (P = no significant difference; Table 1).

Histologic Assessment

Jejunum. Substantial apoptosis in the crypts was observed as early as week 1, progressing through to week 6 (Fig. 1). Villous atrophy was also noted early on in treatment. Goblet cell disintegration was also apparent, becoming very sparse at week 6 (Fig. 1).

Colon. Apoptosis was also prominent in colonic crypts (Fig. 1). Goblet cell composition changed from more acidic to a more neutral mucin. Goblet cell population was also diminishing as treatment progressed (Fig. 1).

Small Intestinal Morphometry

Villus height was significantly decreased in weeks 3 ($P < 0.025$) and 4 ($P < 0.001$) when compared with the controls (Table 2). Intestinal crypt length was significantly increased throughout the 6 weeks of treatment when data were compared with the controls (from week 1 to week 6, all P values were <0.001), whereas mitotic count was significantly decreased from the onset of treatment to week 6 (from week 1 to week 6, all P values were <0.001; Table 2).

Colon Morphometry

In the colon, when compared with the untreated control groups, colonic crypt length was significantly decreased in week 1 of treatment, then becoming significantly increased from week 2 to week 5 of the radiation treatment (from week 1 to week 6, all P values were <0.001; Table 3). At week 6 (P = no significant difference), there was no significant difference in crypt length when compared with controls.

Mitotic counts of the colonic crypts of the untreated controls remained significantly higher than the colonic samples that had been treated with radiation (from week 1 to week 6, all P values were <0.001; Table 3).

Apoptosis

Jejunum. Apoptotic cells peaked at weeks 3 and 5 of treatment (Fig. 2). Throughout the treatment, their numbers were significantly increased when compared with the number of apoptotic cells in the untreated controls (from week 1 to week 6, all P values were <0.001).

Colon. Apoptotic counts from week 1 to week 6 were significantly increased in the colon from the onset of treatment and peaking at week 5 (from week 1 to week 6, all P values were <0.001; Fig. 2). There were generally less apoptotic cells in the colon when compared with the jejunum (Fig. 2).

Immunohistochemical Results

Jejunum. In the small intestine, expression of p53 was localized to the nucleus of the crypt cells, with staining predominantly in the bottom two thirds of the crypt. p53 expression was definitely increased in all irradiated jejunum sections (Fig. 4). There was no expression of p53 in the untreated controls. NF-κB expression was noted throughout the cytoplasm of crypt epithelial cells and surface epithelium and was significantly increased from week 1 to week 6 of treatment when compared with the controls (Figs. 3 and 4).

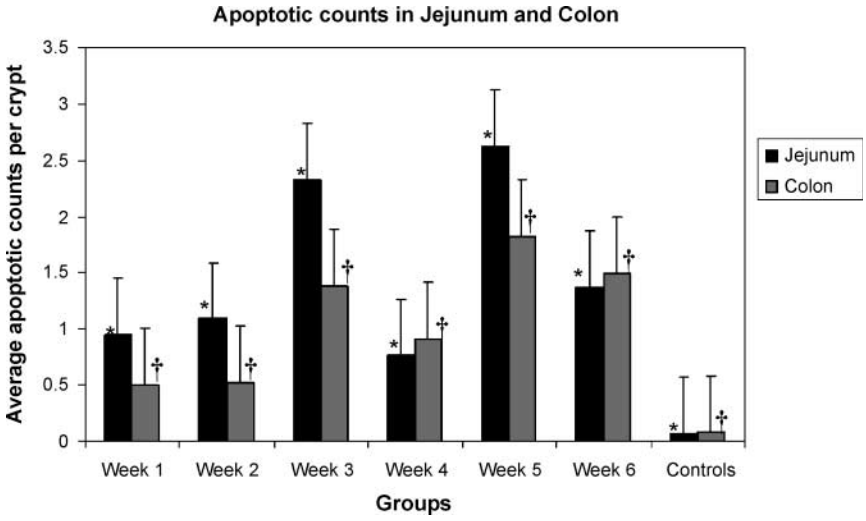

Figure 2. Apoptotic counts in the jejunal and colonic crypts of the Dark Agouti rat at weekly intervals during the 6-w/Fig. 3/ciek fractionated radiation therapy. Controls were untreated. Apoptotic counts in both small and large intestine were significantly increased (* and †, from week 1 to week 6, all P values for Jejunum and Colon were <0.001) in all weeks when compared with the untreated controls.

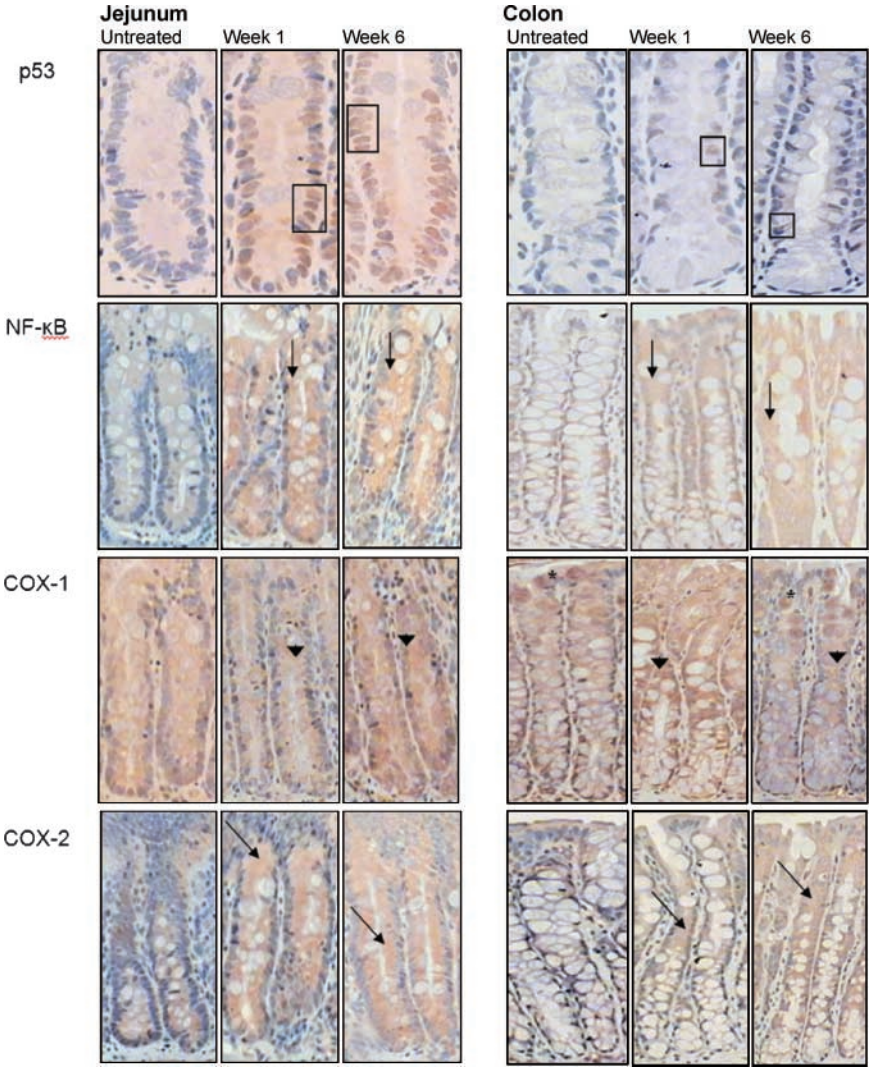

Figure 3. Expression of p53, NF-κB, COX-1, and COX-2 in irradiated jejunum and colon tissue sections from the untreated controls, week 1, and week 6 of radiation therapy. p53 expression was localized to the nuclei of the intestinal crypts in the small and large intestine as indicated by the *boxed nuclei* in the figure and prominently expressed in the irradiated tissue samples. There is a much greater distribution of p53-expressing nuclei in the crypts of the jejunum than in the colon. There was no nuclear p53 expression in the untreated controls. *Straight arrows,* NF-κB expression was increased during the duration of radiation therapy; *arrowheads,* COX-1 expression is slightly increased at the start of treatment, then returning to its basal level equaling that of the untreated controls. *Asterisks,* goblet cells in the intestinal crypts that stained intensely with COX-1. The pattern of COX-2 expression (*slanted arrows*) is similar to that of NF-κB, showing an increased pattern in the cytoplasm of crypt and surface epithelial cells throughout the 6-wk treatment (p53 sections taken at ×200 magnification and NF-κB, COX-1, and COX-2 sections at ×100 magnification).

COX-1 expression in the irradiated jejunum was slightly increased in the first 3 weeks of treatment, and then in the later part of treatment, weeks 5 to 6, expression tapered toward that of the untreated controls (Figs. 3 and 4). COX-1 was noted to be in the cytoplasm of intestinal crypt cells and in the surface epithelial cells. There was also some intense staining of COX-1 in goblet cells in the villi (Fig. 3). COX-2 expression was noted to be within the cytoplasm of epithelial cells lining the crypts, with expression spanning the entire crypt, and in those lining the luminal surface. COX-2 expression was increased from the onset of treatment and progressively increased toward the end of treatment (Fig. 4).

Colon. In the irradiated colon, nuclear staining of p53 in the crypts was increased when compared with no staining in the untreated controls (Fig. 5). The numbers of p53-stained nuclei in the irradiated colonic crypts were less compared with numbers from the irradiated jejunum. This corresponds with the previous TUNEL counts that showed less apoptotic cells in the colon than the jejunum (Fig. 2). There was an increase in NF-κB expression in the irradiated colon when compared with untreated controls. NF-κB was present in increasing amounts toward the end of the 6-week radiation treatment (Figs. 3 and 5). Expression was also noted in the endothelial lining of blood vessels particularly at week 5. COX-1 expression was slightly elevated in weeks 1 to 3 of treatment and then decreased to a basal level to equal the level of expression in the untreated controls (Figs. 3 and 5). COX-1 expression was also detected in the goblet cells present near or at the surface epithelium of the colon in both untreated controls and irradiated sections (Fig. 3). There was a significant increase in COX-2 expression in the cells of the entire colonic crypt and surface epithelium from the onset of treatment when compared with the controls (Figs. 3 and 5).

Discussion

The Dark Agouti rat model is well established for the study of chemotherapy-induced alimentary mucositis (1–4, 25).

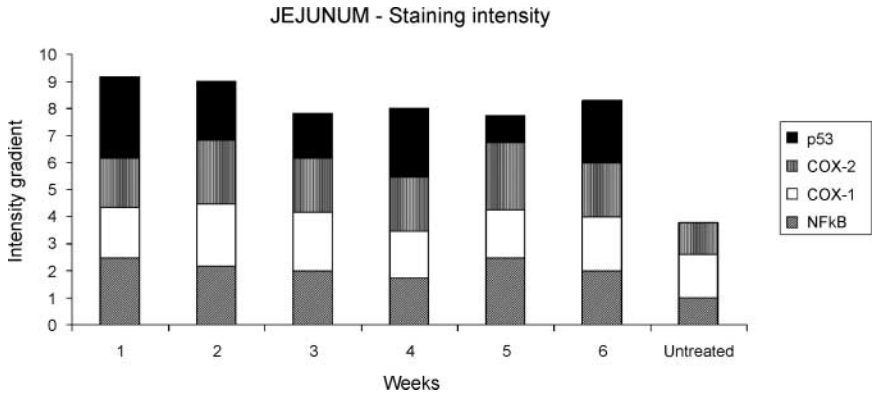

Figure 4. Immunohistochemical expression of p53, NF-κB, COX-1, and COX-2 in irradiated jejunum recorded as intensity of staining. There was a definite increase in p53 expression throughout the treatment, with no expression in untreated controls. NF-κB expression was also significantly increased in all weeks of treatment ($P < 0.05$) when compared with controls. COX-1 expression was slightly increased in the first 3 wks of treatment, then returning to a level similar to that of the untreated controls. COX-2 expression was also increased throughout the treatment but statistically did not produce a significant increase.

This rat model has now been ''adapted'' to study radiation-induced mucositis caused by fractionated radiation therapy. The fractionated schedule used in this study represents a compromise between the more frequent week-daily (five times weekly) dosing in 2 Gy increments in clinical practice and the logistics and risks of having the animals anesthetized more often. Nevertheless, the thrice-weekly dosing in 2.5 Gy increments in the short-term (3 weeks) and long-term (6 weeks) model in the rats corresponds to ~23 Gy in 2 Gy equivalent α/β of 10 and ~50 Gy in 2 Gy equivalent α/β of 3, respectively, based on calculations using the linear quadratic formula, at which dose levels, acute and chronic alimentary mucositis become clinically manifest (26). The sample size was kept at a minimum in this pilot study of the effects of fractionated radiation, and the success of this trial would serve as a basis for larger animal studies.

In this study, the small intestine sustained more severe damage than the large intestine. The hallmark occurrence of apoptosis was apparent early on in treatment in both the small and large intestine, beginning at week 1, continuing throughout the treatment, and peaking by week 5. The increase in apoptosis was accompanied by an increase in expression of nuclear *p53* in the crypts of the small and large intestine affected by radiation. These findings are consistent with our previous studies showing that the earliest effect of chemotherapy is the rise of apoptosis in intestinal crypts (2, 3, 5). Apoptosis is an inherent protective mechanism used by cells to regulate proliferation and occurs at a low level in the healthy, normal small intestine. However, apoptosis is a rare occurrence in the colon (27). In this rat irradiation model, we have shown that the fractionated dosing of ionizing radiation greatly increases the occurrence of apoptosis in both the small and large intestine. This increase in apoptosis was accompanied by an increase in expression of tumor suppressor gene, *p53*, thought to be involved in the recognition of damage in cells and often referred to as the ''guardian'' of the genome. *p53* is usually not widely expressed in the small and large intestine, but its expression was markedly increased on exposure to radiation as shown in this study. Studies by Merritt et al. (27) have shown that the increased expression of *p53* in the irradiated small intestine correlates with the stem cell region, and in the large intestine, the expression of *p53* occurs higher in the crypt, involving more of the proliferative region.

This study also showed that mitotic cell counts were severely depleted within each crypt of the small and large intestine. However, there was a basal level of mitoses occurring possibly due to autoregulation within the stem cell compartment of intestinal crypt cells in response to radiation. It has been reported that the stem cells that survive the ionizing radiation insult become the germinal

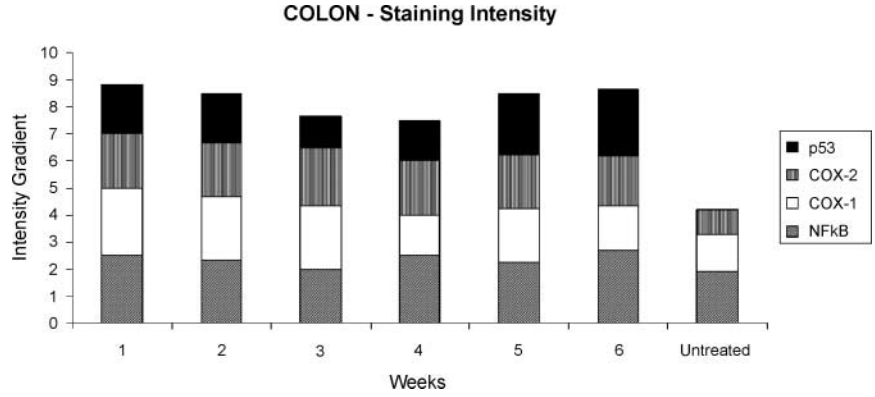

Figure 5. Immunohistochemical expression of p53, NF-κB, COX-1, and COX-2 in irradiated colon recorded as intensity of staining. p53 expression was noted in all treatment groups from week 1 to week 6 and no expression in the untreated group. NF-κB expression was increased from week 1 to week 6 when compared with controls, but this change was not statistically significant. COX-1 was also slightly increased in weeks 1 to 3 of treatment and then returned to basal levels similar to that of untreated samples from week 4 to week 6. COX-2 expression was significantly increased throughout weeks 1 to 6 of treatment when compared with untreated controls ($P < 0.05$).

proliferating tissue compartment, shortening their stem cell cycle and decreasing their rate of terminal differentiation (28). These stem cells could also have accumulated irreversible radiation damage and consequently converted into epithelial cells that line the intestinal luminal surface as a result of migration of their progeny (28). This would result in an alteration in the nature of the epithelial barrier function, which could initiate further mucosal damage as seen in mucositis.

Crypt length of the small and large irradiated intestine was generally increased compared with untreated controls, differing from that seen in the rat model of chemotherapy-induced mucositis where a reduction of crypt length is generally seen (2, 3). The difference might be due to the regenerative response afforded to the epithelial cells of the crypts by the fractionated radiation therapy regimen. The basal level of mitoses as previously discussed contributes to the repopulation effect that occurs after a certain lag period after a dose of ionizing radiation has been delivered (29). This ''rest interval'' between fractionated doses allows for repopulation of cells documented early in the course of radiotherapy (30) and, therefore, might be an explanation as to why there is continuous crypt growth.

The transcription factor *NF-κB* is regarded as the gatekeeper gene, as its activation leads to an up-regulation of >200 genes involved in the mucositis cascade (11, 14, 21, 31, 32). Ionizing radiation is a direct and indirect activator of NF-κB, and this result is confirmed here with a generalized increased expression of NF-κB noted in the intestinal crypt cells, in the surface epithelial cells, and in the endothelial cells of blood vessels. The activation of NF-κB results in the protein transcription of many target genes, among which are the proinflammatory cytokines and cytokine modulators, cell adhesion molecules, acute phase proteins, stress response genes, and cell surface receptors (31). These target genes not only initiate mucosal injury but some also have a role in a positive feedback loop, serving to amplify the primary damage caused by radiation. For example, tumor necrosis factor is not only a proinflammatory cytokine up-regulated by NF-κB but an efficient activator of NF-κB (14, 31). NF-κB also plays a role in the regulation of cell growth and proliferation. This study showed that ionizing radiation increased expression of NF-κB and p53 throughout the 6-week period. The increase in expression may be linked as studies have shown that the induction of *p53* stimulates $pp90^{rsk}$, which activates the RAF/mitogen-activated protein kinase cascade and phosphorylation of inhibitor of κB (33, 34). Activation via this pathway causes a proapoptotic response from NF-κB (33, 34).

This study also confirmed the increased expression of COX-2 in the small and large intestine during the 6-week radiotherapy regimen. COX-2 and NF-κB seemed to follow a similar pattern of expression in this study, with increased expression maintained throughout the duration of the treatment. This finding supports the fact that NF-κB up-regulates the transcription of COX-2, a stress response protein, which in turn leads to the synthesis of prostaglandins involved in the inflammatory cascade resulting in edema and tissue injury (32). In addition, COX-2 contributes to the activation of matrix metalloproteinases, which then cause the breakdown in collagenous subepithelial matrix by matrix metalloproteinase-1 and destruction of the epithelial basement membrane by matrix metalloproteinase-3 (14). This breakdown of the mucosal barrier by matrix metalloproteinase-3 would worsen the hypersecretion of chloride and fluid caused by increased prostaglandins (35). Studies have reported that the role of COX-2 in mucositis may be to increase the severity of mucosal injury and prolong the inflammatory and ulcerative event (21, 36). A recent study has shown that prostaglandin E_2 increase is able to stimulate the transcriptional activity of p53 by a Ser^{15} phosphorylation, subsequently leading to apoptosis (37).

The COX-1 enzyme is responsible for producing homeostatic or maintenance levels of prostaglandins and is constitutively expressed in nearly all normal tissues (35). COX-1 seems to play a major role in the regeneration of the intestinal crypt cells, particularly in the stomach where it maintains proper glandular architecture (35). A study by Cohn et al. (38) showed that crypt stem cell survival in mouse intestinal epithelium is regulated by prostaglandins synthesized through COX-1. That study also showed that irradiation at a single dose of ≥10 Gy results in an increase in COX-1 expression in the intestinal crypt epithelial cells of the mouse. The expression of COX-1 might be up-regulated via a direct effect of radiation injury on stem cells through an indirect effect mediated by radiation-induced cytokine production or through extracellular signaling mechanisms (38). This current study involving a total of 18 fractionated doses of 2.5 Gy showed the up-regulation of COX-1 levels during the early part of the treatment phase, with expression localized to the cytoplasm of the intestinal crypt cells. COX-1 also seemed to be present within goblet cells near the luminal surface in both the jejunum and colon. This may suggest that the role of COX-1 in mediating prostaglandin-dependent gastric protection may not be limited to the gastric mucosa but also play a role in intestinal mucosal protection (39).

This pilot rat study using fractionated radiotherapy has shown that there are complex pathways that lead to the hallmark occurrence of apoptosis in mucositis. The presentation of mucositis in individuals may differ in manifestation of symptoms, clinical signs, and timeline and duration. Factors that may contribute to the diversity of response include the specific region of the alimentary tract affected, the genetics and predisposing factors of the particular individual, and the mode of genetic and cellular insult, which in the case of cytotoxic-induced mucositis includes either chemotherapy or radiotherapy or both. Due to the wide range of gene pathways involved in mucositis, this fractionated radiation animal model is a progressive step toward more foundational studies to further investigate the molecular mechanisms of mucositis so as to

substantiate that which is already known in chemotherapy-induced mucositis research. The development of the fractionated radiotherapy alimentary mucositis model will enhance our ability to compare and contrast chemotherapy- and radiotherapy-induced damage to the alimentary tract, which will enable development of targeted antimucotoxic therapies.

Acknowledgments

We thank the Department of Radiation Oncology (Royal Adelaide Hospital) for their technical help; the Animal House staff at the Institute of Medical and Veterinary Science, Adelaide, for their assistance during the running of this animal study; Dr. John Finnie for expert histopathologic opinion; and Dr. Tim Kuchel for veterinary advice.

References

1. Gibson RJ. Chemotherapy-induced mucositis: mechanisms of damage, time course of events and possible preventative strategies. Adelaide: Department of Medicine, University of Adelaide; 2004. p. 129.

2. Gibson RJ, Bowen JM, Cummins AG, Keefe DM. Relationship between dose of methotrexate, apoptosis, p53/p21 expression and intestinal crypt proliferation in the rat. Clin Exp Med 2005;4:188 – 95.

3. Gibson RJ, Bowen JM, Inglis MR, Cummins AG, Keefe DM. Irinotecan causes severe small intestinal damage, as well as colonic damage, in the rat with implanted breast cancer. J Gastroenterol Hepatol 2003;18: 1095 – 100.

4. Gibson RJ, Keefe DM, Thompson FM, et al. Effect of interleukin-11 on ameliorating intestinal damage after methotrexate treatment of breast cancer in rats. Dig Dis Sci 2002;47:2751 – 7.

5. Keefe DM, Brealey J, Goland GJ, Cummins AG. Chemotherapy for cancer causes apoptosis that precedes hypoplasia in crypts of the small intestine in humans. Gut 2000;47:632 – 7.

6. Bowen JM, Gibson RJ, Cummins AG, Tyskin A, Keefe DM. Irinotecan changes gene expression in the small intestine of the rat with breast cancer. Cancer Chemother Pharmacol 2007;59:337 – 48.

7. Logan RM, Gibson RJ, Sonis ST, Keefe DM. Nuclear factor-κB (NF-κB) and cyclooxygenase-2 (COX-2) expression in the oral mucosa following cancer chemotherapy. Oral Oncol 2007;43:395 – 401.

8. Bowen JM. Expression of Bcl-2 family members in the small and large intestine. Adelaide: Department of Gastroenterology and Hepatology, University of Adelaide; 2001. p. 49.

9. Bowen JM, Gibson RJ, Cummins AG, Keefe DM. Intestinal mucositis: the role of the Bcl-2 family, p53 and caspases in chemotherapy-induced damage. Support Care Cancer 2006;14:713 – 31.

10. Bowen JM, Gibson RJ, Keefe DM, Cummins AG. Cytotoxic chemotherapy upregulates pro-apoptotic Bax and Bak in the small intestine of rats and humans. Pathology 2005;37:56 – 62.

11. Blijlevens N, Sonis S. Palifermin (recombinant keratinocyte growth factor-1): a pleiotropic growth factor with multiple biological activities in preventing chemotherapy- and radiotherapy-induced mucositis. Ann Oncol 2007;18:817 – 26.

12. Saadi S, Holzknecht RA, Patte CP, Stern DM, Platt JL. Complement-mediated regulation of tissue factor activity in endothelium. J Exp Med 1995;182:1807 – 14.

13. Sonis ST. Pathobiology of mucositis. Semin Oncol Nurs 2004;20: 11 – 5.

14. Sonis ST. The pathobiology of mucositis. Nat Rev Cancer 2004;4: 277 – 84.

15. Keefe DM. Gastrointestinal mucositis: a new biological model. Support Care Cancer 2004;12:6 – 9.

16. Keefe DM, Gibson RJ, Hauer-Jensen M. Gastrointestinal mucositis. Semin Oncol Nurs 2004;20:38 – 47.

17. Pico JL, Avila-Garavito A, Naccache P. Mucositis: its occurrence, consequences, and treatment in the oncology setting. Oncologist 1998;3: 446 – 51.

18. Kushwaha RS, Hayne D, Vaizey CJ, et al. Physiologic changes of the anorectum after pelvic radiotherapy for the treatment of prostate and bladder cancer. Dis Colon Rectum 2003;46:1182 – 8.

19. Yeoh EK, Russo A, Botten R, et al. Acute effects of therapeutic irradiation for prostatic carcinoma on anorectal function. Gut 1998;43:123 – 7.

20. Wilkes JD. Prevention and treatment of oral mucositis following cancer chemotherapy. Semin Oncol 1998;25:538 – 51.

21. Yeoh AS, Bowen JM, Gibson RJ, Keefe DM. Nuclear factor κB (NFκB) and cyclooxygenase-2 (Cox-2) expression in the irradiated colorectum is associated with subsequent histopathological changes. Int J Radiat Oncol Biol Phys 2005;63:1295 – 303.

22. Krajewska M, Wang HG, Krajewski S, et al. Immunohistochemical analysis of *in vivo* patterns of expression of CPP32 (caspase-3), a cell death protease. Cancer Res 1997;57:1605 – 13.

23. Krajewski S, Krajewska M, Reed JC. Immunohistochemical analysis of *in vivo* patterns of Bak expression, a proapoptotic member of the Bcl-2 protein family. Cancer Res 1996;56:2849 – 55.

24. Krajewska M, Zapata JM, Meinhold-Heerlein I, et al. Expression of Bcl-2 family member Bid in normal and malignant tissues. Neoplasia 2002; 4:129 – 40.

25. Gibson RJ, Bowen JM, Keefe DM. Palifermin reduces diarrhea and increases survival following irinotecan treatment in tumor-bearing DA rats. Int J Cancer 2005;116:464 – 70.

26. Yeoh E, Horowitz M, Russo A, et al. Effect of pelvic irradiation on gastrointestinal function: a prospective longitudinal study. Am J Med 1993;95:397 – 406.

27. Merritt AJ, Potten CS, Kemp CJ, et al. The role of p53 in spontaneous and radiation-induced apoptosis in the gastrointestinal tract of normal and p53-deficient mice. Cancer Res 1994;54:614 – 7.

28. Dorr W. Three A's of repopulation during fractionated irradiation of squamous epithelia: asymmetry loss, acceleration of stem-cell divisions and abortive divisions. Int J Radiat Biol 1997;72:635 – 43.

29. Dorr W. Modulation of repopulation processes in oral mucosa: experimental results. Int J Radiat Biol 2003;79:531 – 7.

30. Fowler JF. Rapid repopulation in radiotherapy: a debate on mechanism. The phantom of tumor treatment-continually rapid proliferation unmasked. Radiother Oncol 1991;22:156 – 8.

31. Sonis ST. The biologic role for nuclear factor-κB in disease and its potential involvement in mucosal injury associated with anti-neoplastic therapy. Crit Rev Oral Biol Med 2002;13:380 – 9.

32. Yeoh A, Gibson R, Yeoh E, et al. Radiation therapy-induced mucositis: relationships between fractionated radiation, NF-κB, COX-1, and COX-2. Cancer Treat Rev 2006;32:645 – 51.

33. Ryan KM, Ernst MK, Rice NR, Vousden KH. Role of NF-κB in p53-mediated programmed cell death. Nature 2000;404:892 – 7.

34. Ryan KM, Phillips AC, Vousden KH. Regulation and function of the p53 tumor suppressor protein. Curr Opin Cell Biol 2001;13:332 – 7.

35. Dubois RN, Abramson SB, Crofford L, et al. Cyclooxygenase in biology and disease. FASEB J 1998;12:1063 – 73.

36. Sonis ST, O'Donnell KE, Popat R, et al. The relationship between mucosal cyclooxygenase-2 (COX-2) expression and experimental radiation-induced mucositis. Oral Oncol 2004;40:170 – 6.

37. Faour WH, He Q, Mancini A, et al. Prostaglandin E2 stimulates p53 transactivational activity through specific serine 15 phosphorylation in human synovial fibroblasts. Role in suppression of c/EBP/NF-κB-mediated MEKK1-induced MMP-1 expression. J Biol Chem 2006;281: 19849 – 60.

38. Cohn SM, Schloemann S, Tessner T, Seibert K, Stenson WF. Crypt stem cell survival in the mouse intestinal epithelium is regulated by prostaglandins synthesized through cyclooxygenase-1. J Clin Invest 1997;99:1367 – 79.

39. Jackson LM, Wu KC, Mahida YR, Jenkins D, Hawkey CJ. Cyclo-oxygenase (COX) 1 and 2 in normal, inflamed, and ulcerated human gastric mucosa. Gut 2000;47:762 – 70.

Molecular Cancer Therapeutics

A novel animal model to investigate fractionated radiotherapy-induced alimentary mucositis: the role of apoptosis, p53, nuclear factor-κB, COX-1, and COX-2

Ann S.J. Yeoh, Rachel J. Gibson, Eric E.K. Yeoh, et al.

Mol Cancer Ther 2007;6:2319-2327.